A hybrid reed instrument: an acoustical resonator with a numerically simulated mouthpiece

Kurijn Buys, Christophe Vergez

ACOUSTICS 2012

A hybrid reed instrument: an acoustical resonator with a numerically simulated mouthpiece

K. Buys and C. Vergez

LMA - CNRS (UPR 7051), 31 chemin Joseph-Aiguier, 13402 Marseille, Cedex 20, France
kurijn@gmail.com

A study on the development of a hybrid wind instrument is carried out. An acoustical tube interacts with a numerically simulated mouthpiece in real-time, with the aim to propose in the long term both a tool for objective measurements, and a new musical instrument, easily playable, with unique timbral capacities. This preliminary study focusses on a first prototype, to verify the physical meaningfulness and estimate its potential. A microphone at the tube entrance feeds a numerical model of the reed used to compute the volume flow through the reed channel. This is the output of the numerical part, which is directed to an electrovalve that proportionally modulates the volume flow between the compressed air source and the tube entrance. The hybrid instrument is characterized by studying its parts separately (evaluation of the electrovalve characteristics, impedance measurement of the resonator), but also as a whole by analyzing its behaviour when the parameters of the mouthpiece are varied. Both transients and steady regimes are compared to a fully simulated instrument. We observe a coherent functioning for fundamental frequencies sufficiently below the electrovalve's first resonant frequency. The foremost drawbacks are associated to the electrovalve's mechanics and to noisy pressure measurements.

1 Introduction

The idea to replace a wind instrument's exciter by a numerical simulation is motivated by two main roots: research and creation.
In the same regard as the artificial mouth for wind instruments, this device would allow studying the instrument by a more controllable approach. In this case the mouthpiece model and parameters are exactly known, which would provide a precise research device if appropriate transducers can be found.
The creative motives are straightforward: such a combination offers interesting potentials for the direct use of the sound in a musical context. One could think of simply adapting the mouthpiece model with arbitrary parameters, varying them over time or adapting the model itself.
The great difficulty for this device are the transducers that make the link between the two worlds, as they're expected to act in an objective way to the demands of the simulation. The feasibility also depends on the total latency, the stability of the system, the demanded amount of energy and up till which frequency the communication has to occur. This explains why such hybrid systems are still unknown today, and why we preliminary study a low frequency behavior by using a long tube for the resonator.
The global working of the hybrid system is represented in figure 1 on the left, and is as follows: the pressure just after the electrovalve is measured by a small microphone and send to the simulation of the mouthpiece, implemented on a digital processor board. Then, the calculated flow rate corresponding to the simulated mouthpiece is directed to the actuator in real time. Finally, together with the resonator's response a new pressure is measured by the microphone, to form a looped system.
In the next section we will briefly describe the theoretical models of a single reed mouthpiece and a cylindrical bore, to then study the hybrid prototype by both a characterizing and a phenomenological approach.

2 Theoretical models

2.1 The mouthpiece

On the right of figure 1, an outline of a woodwind mouthpiece is depicted, with indications corresponding to the used model. We adopted a typical physical model from Chaigne and Kergomard [1, Chapt. 9]. For simplicity, the mouthpiece is modeled with a quasistatic reed, i.e. neglecting it's dynamical properties.

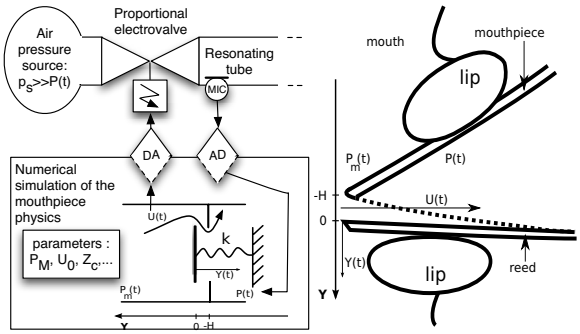

Figure 1: Left: Flow diagram representing the functioning of the hybrid wind instrument. Right: outline of a mouthpiece with a mouth in playing position.

2.1.1 The reed displacement

In this approach, the reed position is governed by the surrounding pressure difference between mouth and mouthpiece pressure: $\Delta P = P_m - P$, which acts on S_r, the "effective" part of the reed surface, and creates a force according to the reed position Y and stiffness k_r (which includes the player's lip). This results in the following equation:

$$-S_r \Delta P = k_r Y. \tag{1}$$

The reed position is taken relative to its distance H from the mouthpiece tip when the reed is at rest and no mouth pressure is applied. We say that the reed "beats", when it touches the tip, which happens at $Y = -H$ and at the pressure difference $P_M = \frac{k_r H}{S_r}$ and above. Introducing $y = Y/H$ for the reed position, $p = P/P_M$ for the mouthpiece pressure, and $\gamma = P_m/P_M$ for the mouth pressure, we may nondimensionalize equation 1 to become:

$$y = p - \gamma. \tag{2}$$

2.1.2 The flow passing through the reed channel

The reed creates an opening or "channel" to the bore entrance that allows an air flow to enter the instrument, expressed as the product of the flow velocity v_f and the effective reed opening section S_f. The former can be found by the Bernoulli theorem applied between the mouth and the reed channel and the latter is supposed linearly related to the reed displacement [2]. The resulting flow rate can be expressed as:

$$U = \underbrace{sign(\Delta P)\sqrt{\frac{2|\Delta P|}{\rho}}}_{v_f} \underbrace{\mathcal{H}(Y+H)(Y+H)w}_{S_f}, \tag{3}$$

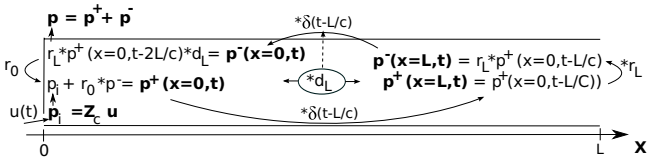

Figure 2: Schematic representation of half open tube and the incomming, up- and downstream pressure calculations.

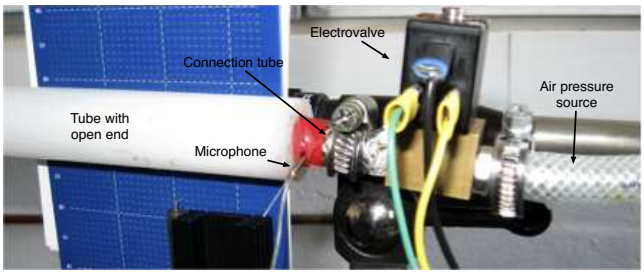

Figure 3: Picture of the experimental set-up of the hybrid instrument with indications.

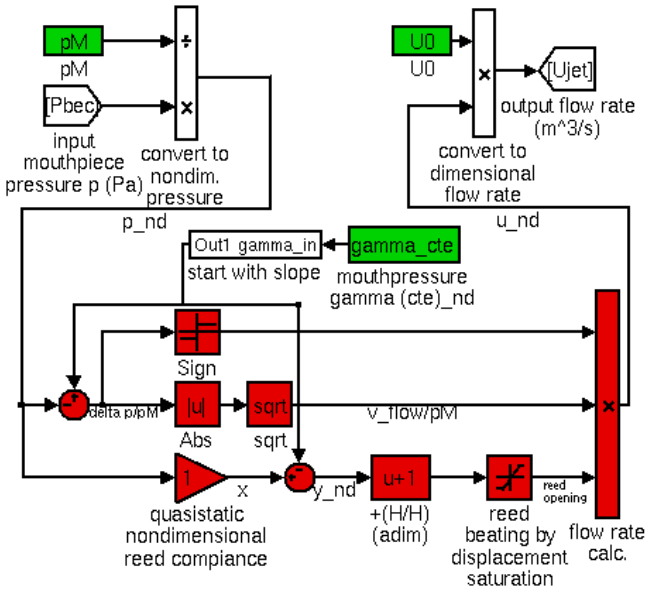

Figure 4: The Simulink block diagram of the mouthpiece simulation.

where $\rho = 1.204\,kg/m^3$ designates the air density and w the effective reed width. The *sign* operator is introduced to make the calculation of negative flows possible and the Heaviside function $\mathcal{H}$ to hold a zero flow rate when the reed is beating. The input impedance of the resonator is very low for continuous flows, so we can suppose $Z_{entr}(\omega = 0) = 0$, and thus may assume a constant mouth pressure P_m [1].
We note that the maximum flow rate that enters the bore is obtained at a pressure difference of $\Delta P = \frac{P_M}{3}$ and amounts:

$$U_{max} = U_0 \frac{2}{3\sqrt{3}}, \tag{4}$$

where $U_0 = wH\sqrt{\frac{2}{\rho}P_M}$. We also use this value to nondimensionalize the flow rate: $u = U/U_0$, so that equation 3 becomes:

$$u = sign(\gamma - p)\sqrt{|\gamma - p|}\mathcal{H}(y+1)(y+1). \tag{5}$$

2.2 The bore

In order to compare the hybrid instrument with an entirely simulated clarinet, we use a physical model of a cylindrical acoustic bore. The model consists of a temporal calculation of the up- and downstream pressure flows, similarly to the theory presented by McIntyre, et all. [3]. The governing equations are presented in figure 2. The model comprises a single real dissipation factor d_L (derived later on), based on a model by Kirchhoff [4], without the small imaginary part and frequency influence, and a simplified complex reflexion function r_L at the open end, adopted from Silva et all. [5]. At the bore entrance, a Neumann condition is supposed so that $r_0 = \delta(t)$. We further don't detail this theory here, as it is out of the scope of this paper.

3 Study of a hybrid prototype

3.1 Realization

The main part of the constructed hybrid prototype is shown in figure 3. It is build with a PVC tube with an inner section radius of 7.1 *mm* and a short tube with a smaller section that connects the resonator to a Bürkert *2824* electrovalve. The total tube length is chosen long enough to ensure a reasonable electrovalve performance (i.e. with a playing frequency far below the electrovalve resonance frequency). A small *Endevco* piezoresistive microphone is inserted in the tube, close enough to the electrovalve output. Since we use a constant input pressure of 3.8 *bar*, we use the valve in its supercritical domain where the flow rate becomes proportional to the input current. The chosen flow mechanism excludes the simulation of negative airflows. However, in practice such flows are rarely occurring and even if they do the amplitudes are small [1]. The real-time mouthpiece simulation is performed by a *dSpace* interface with processor board DS1006, which we configured at a 50 *kHz* maximum sample rate with a fixed time-step Runge-Kutta solver. The numerical implementation has been realized in MATLAB and Simulink, which can directly be loaded to this interface. Figure 4 shows the functional scheme of the mouthpiece model implemented in Simulink. Firstly, the incoming pressure signal, either comming from the microphone or the simulated tube pressure, is nondimensionalized by P_M. Next, equations 2 and 5 are applied to obtain the nondimensional flow rate, which is then multiplied by U_0 to become a dimensional flow rate that is either send to the electrovalve or to the tube simulation.

3.2 Characterizing study

3.2.1 Noise due to a turbulent flow

As the microphone in the hybrid set-up ought to be positionned next to the electrovalve output, it receives a notable level of noise due to flow turbulence. An experimental evaluation of an increasing input flow rate revealed an exponential relation of the measured pressure gain, which might explain the limited hybrid auto-oscillating functioning for high flow rates, found empirically.

3.2.2 Electrovalve flow rate study

The electrovalve's characteristics account for the predominant side effects of the hybrid device. It's mechanical aspects are the least apropriate to the rapid dynamic demands of

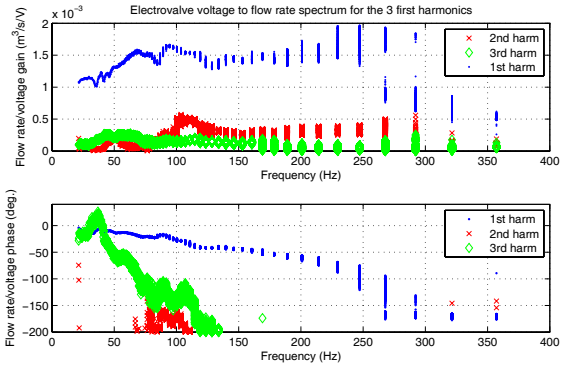

Figure 5: Electrovalve flow rate per voltage spectrum for the three first harmonics.

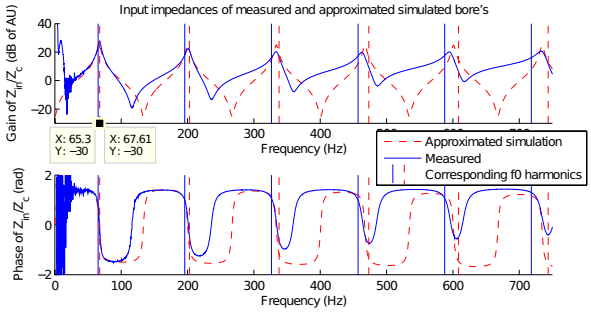

Figure 6: Spectral input impedances of the measured and approximated simulated tube.

this application which motivates this brief qualifying study.
The used electrovalve needs an initial voltage offset before a flow output is attained, and further knows dynamic, hysteretic and nonlinear characteristics. Ferrand and Vergez [6] have examined a similar electrovalve of the type *2832*, and found a resonant frequency of about 240 Hz.
We investigated a dynamic study of the flow rate response in relation to a sinusoidal voltage input. We used a seven meter long tube with a microphone in the midle to obtain a desired flow measurement device. Firstly, the relation between the flow rate at the entrance and the pressure at the microphone is measured with an acoustic impedance sensor [7]. Next, the electrovalve is mounted on the tube and the Fourier transform of the measured pressure is devided by the previous relation to obtain the flow rate. The tube length is chosen in order to ensure an impedance whose spectral gain has a sufficiently high mean and low variance value in the frequency domain of our interest. Choosing a long tube has another advantage: the electrovalve flow turbulence cancels out enough before reaching the microphone. To add the missing flow offset in this measurement, an additional low speed mass flow meter is mounted before the electrovalve.
We evaluated the flow rate for a 100 mV sine sweep and a 0.175 V offset. The spectral result presented in figure 5 shows the gain and phase of the three first harmonics of the flow rate to input voltage ratio. The second and third harmonics are worth only about a fifth, and a tenth of the first harmonic's gain. Whereas the second harmonic is not present in the case of the clarinet, this nonlinear characteristic might possibly raise it's presence in the hybrid clarinet.
Given the slowly progressive phase, the presence of hysteresis and the reduced flow regime jump, it is not straigthforward to estimate the resonant frequency of the valve, but we can confirm that it is arround 240 Hz where a phase of $-90°$ is found.
We also evaluated a 200 mV sine sweep and obtained a fairly similar result. However, we noted that starting from such amplitudes and also for higher voltage offsets, often ambiguous oscillation regimes were obtained, such as sudden amplitude changes and the appearing of an additional subharmonic oscillation, which might explain the experienced difficulties to empirically attain auto-oscillations with the hybrid prototype for higher voltage values. We also note that in each case the flow regime jumps to a fairly reduced amplitude when the sine wave frequency exceeds about 270 Hz.
A fully characterising analysis of the electrovalve is not in the scope of this study, we rather use these findings to obtain an optimal functional hybrid instrument and to interpret it's behavior later on.
We might consider to perform an inverse processing on the calculated flow rate signal before sending it to the electrovalve, but given the negative phases it would demand a non-causal operation. Therefore, we only use a static gain, derived by averaging the gain of the first harmonic in the frequency domain of our interest, between 60 and 260 Hz. We obtain a value of $1.53 \cdot 10^{-3}\, m^3/s/V$, which is not far from it's equivalent static ratio, found at $1.34 \cdot 10^{-3}\, m^3/s/V$.
The global result seems to be satisfying for a use in the low frequency domain where the amplitude response is reasonably constant and the phase deviation is very progressive. Obviously, we're far from the ideal actuator but this quantizing study will also allow a reflexion on the choice of a future actuator.

3.2.3 Calibration of the bore model

In the next section, a phenomenological study is performed by comparing the hybrid and entirely simulated instrument. In order to make this comparison usefull for interpreting the influence of the transducers, the simulated and physical bore impedances should match to a certain extent. We compared the concerning spectral impedance curves and tuned the tube length parameter L and the tube losses factor d_L to make them as close as possible. The result is shown in figure 6, as well as the harmonics of the simulated and the hybrid fundamental frequencies derived during experimental auto-oscillation. These harmonics indicate the exact gain and phase on their corresponding impedance curves. The first harmonic of both models matches properly, the second and third harmonics indicate a 2 dB lower gain for the measured impedance, and an equal but opposite phase difference compared to the simulated tube's phase, which evokes an equal gain reduction. Starting from the fourth harmonic, more important phase and gain differences are found. The approximation is found for $L = 1.284\, m$ and $d_L = 0.896$. It may be noted that the short connection tube at the entrance (cf. fig. 3) explains the increasing measured impedance gain.

3.3 Phenomenological study

3.3.1 Auto-oscillating domain

An interesting method to verify the hybrid instrument's performances, is to evaluate it for different values of P_M and U_0 while holding the same parameters of the nondimensional model. Since these factors directly control the in- and

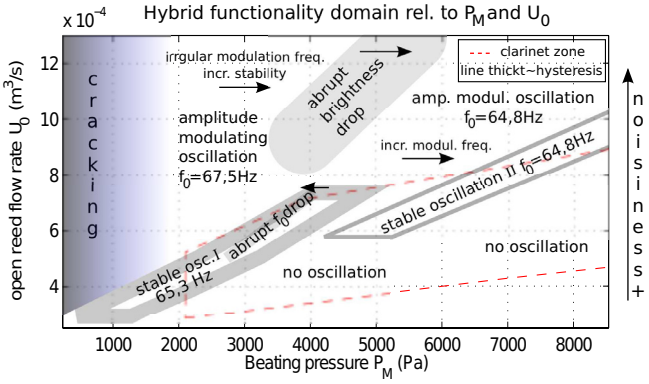

Figure 7: Hybrid functionality domain relative to P_M and U_0 for $\gamma = 0.5$. The dashed line indicates the typical domain of functioning for clarinets.

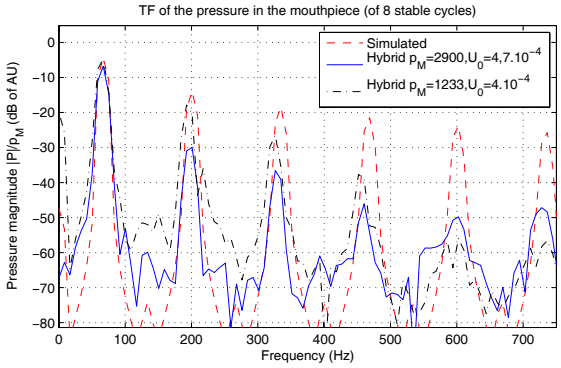

Figure 8: Comparison between the simulated and two hybrid mouthpiece pressure spectral gains for $\gamma = 0.5$.

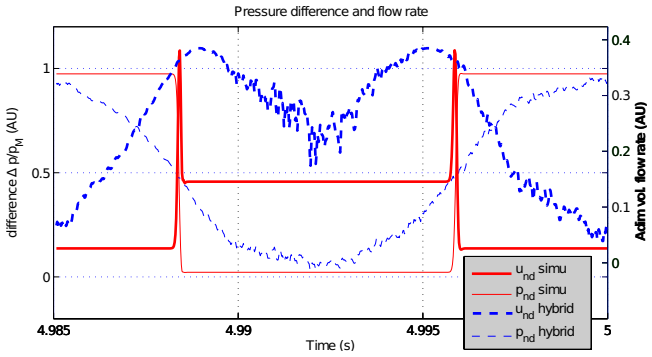

Figure 9: Temporal pressure and corresponding calculated flow rate signal for $\{P_M = 2900\,Pa, U_0 = 4.7 \cdot 10^{-4}\,m^3/s\}$ and $\gamma = 0.5$.

output to the physical part, the interpretation will be more straightforward than an evaluation of specific reed parameter variations. Figure 7 shows this domain for γ maintained at 0.5. Higher γ values result in larger auto-oscillation domains, but this value indicates more precisely the most sturdy zones. The result shows several specific behaviors which often occur with an important hysteresis in relation to P_M and U_0. The encountered abrupt slight brightness and fundamental frequency drops may be related to the ambiguous regime changes found in the discussed electrovalve study since they occur for $U_0 \geq 4.5 \cdot 10^{-4}\,m^3/s$, which corresponds to maximum flow rates of $U_{max} \geq 1.7 \cdot 10^{-4}\,m^3/s$ (using equation 4) or electrovalve voltages that surpass $120\,mV$. A wide zone results in amplitude modulating (rhythmical beating) oscillations, further two small stable oscillation zones are observed. It is interesting to note that they mark a zone with a low P_M/U_0 variation. For a constant P_M/U_0 ratio the simulated nondimensional result, and thus the signal shape, remains equal, which means that the hybrid instrument especially seems capable to perform a certain specific signal, to a certain extent regardless of the amplitude.

On the same figure, we plotted a zone (dashed line) with typical P_M and U_0 combinations for clarinets. We took the jet effective width between $w = 12 - 18\,mm$, the reed's initial opening $H = 0.3 - 1.0\,mm$, its stiffness per effective surface may be considered as about constant between $k/S_r = (0.7 - 1.3) \cdot 10^7\,N/m^2$. These are based on extremities of the mouthpiece parameters as found in several writings: Fletcher [8], Dalmont et al. [2] and Avanzini and van Walstijn [9]. It is interesting to note that a substantial part of the hybrid stable oscillation zones lies inside the typical reed instrument domain.

We selected a few stable hybrid auto-oscillating states ($\{P_M, U_0\}$ pairs) and compared their signals (all found with a fundamental frequency of $f_0 = 65.3\,Hz$) with the corresponding simulated signals. Figure 8 shows the spectral gains of the pressure signals obtained by the hybrid instrument for $\{P_M = 2900\,Pa, U_0 = 4.7 \cdot 10^{-4}\,m^3/s\}$ and $\{P_M = 1233\,Pa, U_0 = 4 \cdot 10^{-4}\,m^3/s\}$ and by the simulated instrument (the simulated instrument's spectrum for the whole stable hybrid oscillation zone is as good as equal). At other states in this stable zone the spectrum resembled to the second hybrid curve, which at first sight confirms a better approximation to the simulation. However the temporal pressure and flow rate signals revealed a beating reed behavior for these states, contrary to the first state's and simulated pressure signals that just don't reach the beating regime, as it should happen for this γ value. Furthermore, the first state seems more repeatable and robust for γ variations, so that we elected this state for the further study. Figure 9 shows the temporal pressure and corresponding calculated flow rate for this state for $\gamma = 0.5$. It is clearly visible that the electrovalve's dynamics have an important influence on the signal, as the calculated flow rate (which is not the actual realized flow rate) shows a remarkable low-pass filtered response compared to the simulated flow rate signal. When the measured pressure approaches the mouth pressure value, visibly the noise has a considerable influence on the flow rate calculation.

The second stable oscillation zone ($f_0 = 64.8\,Hz$) resulted in a fairly different oscillation for both numerical and hybrid models. This is due to the higher P_M/U_0 ratio, which brings the oscillation threshold closer to P_M [10], so that for $\gamma = 0.75$, a downward-sloping spectral envelope is found for both models. However the hybrid oscillations maintain amplitudes close to P_M, while the simulation's amplitude lies about $50\,dB$ under this pressure! We suppose that in this zone, the electrovalve mechanical aspects might play an advantageous role to uphold a strong oscillation regime that is not proper to the typical quasistatic clarinet model.

3.3.2 RMS mouthpiece pressure in relation to the mouth pressure

Dalmont et al. [10] and Karkar et al. [11] demonstrated a bifurcating evolution of the RMS or quadratic meaned mouthpiece pressure in function of the mouth pressure. The selected hybrid state at $\{P_M = 2900\,Pa, U_0 = 4.7 \cdot 10^{-4}\,m^3/s\}$ has been examinated for different γ values, which directly control the mouthpiece pressure for a constant P_M. We applied an additional small dither signal to the electrovalve in

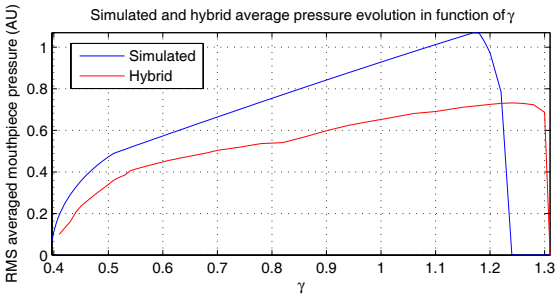

Figure 10: Simulated and hybrid RMS pressure evolution in function of γ, for $P_M = 2900\,Pa$ and $U_0 = 4.7 \cdot 10^{-4}\,m^3/s$.

order to effectively lower the hysteretic characteristics when the system is close to stable, so that a lower hybrid oscillation threshold can be reached. This added signal slightly increases the measured RMS pressure, but only in the order of $0.02 \cdot P_M\,Pa$. Figure 10 shows both RMS pressure diagrams. The diagram of the simulated instrument closely corresponds to the theoretical approach pointed out by Dalmont et al.[10], where an equal model is studied except from a global real total acoustic losses parameter, while our model includes a complex radiation function. The simulated oscillation threshold is found at $\gamma = 0.397$ and the hybrid one at $\gamma = 0.41$. However, it seems that if the electrovalve hysteresis would be absent, the threshold would fall at the same threshold as the simulation. It is further remarkable that the hybrid diagram shows a coherent evolution, as we can distinguish a beating and nonbeating reed regime (where the former corresponds to the more linear part of the curve). The globally reduced hybrid mouthpiece pressure is explainable by the steeper spectral gain decrease (cf. fig 8), which lowers the RMS pressure without reducing the peak-to-peak pressure amplitude that is more adequat for auto-oscillating systems. It may be of interest later on to reveal the bifurcation diagrams for other tube lengths to verify the influence of the electrovalve dynamical properties, which represent probabely the main drawback of this first hybrid prototype.

4 Conclusions

Using a quasistatic mouthpiece model programmed on a *dSpace* DSP interface, a $1.3\,m$ long tube with a microphone at the entrance and a Bürkert *2824* electrovalve, a first prototype of a hybrid wind instrument has been constructed.
A characterizing study revealed certain qualitative aspects of the used components, such as an exponentially increasing measured noise level with the electrovalve flow rate, and a dynamical slightly nonlinear electrovalve response. The latter seems to be repeatable for input sine waves with gains up till $100\,mV$ and frequencies up till $270\,Hz$, using a voltage offset of $0.175\,V$ and a $3.8\,bar$ input pressure. A physical model of a cylindrical bore has been calibrated to the measured impedance
Keeping in mind these findings, we evaluated a phenomenological study on the hybrid clarinet functioning. Despite of a rather rough pressure signal and a probable important dynamic influence around $240\,Hz$, a limited but existing $\{P_M, U_0\}$ auto-oscillating zone with a coherent harmonics spectrum at a fundamental frequency of $65.3\,Hz$ is found. An evaluation of the mouth pressure revealed a typical evolution of the RMS mouthpiece pressure.

This result guides us to a next more thorough research for a suitable electrovalve and hybrid instrument set-up that will be capable of serving as both a research and a musical tool. As for next hybrid prototype perspectives, special attention should be given to an electrovalve with the least possible dynamics and hysteresis.

Acknowledgements

This work is supported by the french *Agence Nationale de la Recherche* within the framework of the project SDNS-AIMV.

References

[1] A. Chaigne and J. Kergomard, *Acoustique des instruments de musique*, Belin, Paris, France, 2008.

[2] J.-P. Dalmont, J. Gilbert and S. Ollivier, "Nonlinear characteristics of single-reed instruments: Quasistatic volume flow and reed opening measurements," *J. Acoust. Soc. Am.*, vol. 114, pp. 2253-2262, Oct. 2003.

[3] M. E. McIntyre, R. T. Schumacher and J. Woodhouse, "On the oscillations of musical instruments", *Journal of the Acoustical Society of America*, vol. 74, pp. 1325-1345, Nov. 1983.

[4] G. Kirchffoff, "Ueber den Einfluss der Wärmeleitung in einem Gase auf die Schallbewegung". *Annalen der Physik Leipzig*, 134:177-193, 1868.

[5] F. Silva, J. Kergomard and C. Vergez, "Interaction of reed and acoustic resonator in clarinetlike systems", *Journal of the Acoustical Society of America*, 124(5):3284-95, 2008.

[6] D. Ferrand, C. Vergez, B. Fabre and F. Blanc, "High-Precision Regulation of a Pressure Controlled Artificial Mouth: The Case of Recorder-Like Musical Instruments", *Acta Acustica united with Acustica*, 96(4): p. 701-712, 2010.

[7] C. A. Macaluso and J.-P. Dalmont, "Trumpet with near-perfect harmonicity: Design and acoustic results", *J. Acoust. Soc. Am. 129(1)*, 404?414, 2011.

[8] N. H. Fletcher, "Excitation Mechanisms in Woodwind and Brass Instruments," *Acustica*, 43(1), pp. 63-72, 1979.

[9] F. Avanzini and M. van Walstijn, "Modeling the Mechanical Response of the Reed-Mouthpiece-Lip System of a Clarinet. Part I. A One-Dimensional Distributed Model", *Acta Acustica united with Acustica.*, Vol. 90, pp. 537-547, 2004.

[10] J.P. Dalmont, J. Gilbert, J. Kergomard and S. Ollivier, "An analytical prediction of the oscillation and extinction thresholds of a clarinet", *J. Acoust. Soc. Am. 118*, 2005.

[11] S. Karkar, C. Vergez and B. Cochelin, "Exploration systématique des régimes périodiques des instruments à anche", *10ème Congrès Français d Acoustique*, Lyon, France, 2010.